Variability in the durability of CRISPR-Cas immunity

Hélène Chabas[1], Antoine Nicot[1], Sean Meaden[2], Edze Westra[2], Denise Tremblay[3,4], Léa Pradier[1], Sébastien Lion[1], Sylvain Moineau[3,4] and Sylvain Gandon[1]

[1]CEFE UMR 5175, CNRS – Université de Montpellier – Université Paul-Valéry Montpellier – EPHE, 1919, route de Mende, 34293 Montpellier Cedex 5, France
[2]Environment and Sustainability Institute, University of Exeter, Penryn Campus, Penryn, Cornwall, TR10 9FE, UK
[3]Département de biochimie, microbiologie et de bio-informatique, Faculté des sciences et de génie, Université Laval, 1045 avenue de la Médecine, Québec City, QC, Canada, G1V 0A6
[4]Félix d'Hérelle Reference Center for Bacterial Viruses and Groupe de recherche en écologie buccale, Faculté de médecine dentaire, Université Laval, Québec City, QC, Canada, G1V 0A6

Keywords: Durability of resistance, pathogen evolution, CRISPR-Cas, mutation rates

Abstract

The durability of host resistance is challenged by the ability of pathogens to escape the defense systems of their hosts. Understanding the variability in the durability of host resistance is of paramount importance for designing more effective control strategies against infectious diseases. Here we study the durability of various CRISPR-Cas alleles of the bacteria *Streptococcus thermophilus* against lytic phages. We found substantial variability in durability among different resistant bacteria. Since the escape of the phage is driven by a mutation in the phage sequence targeted by CRISPR-Cas, we explored the fitness costs associated with these escape mutations. We found that, on average, escape mutations decrease the fitness of the phage. Yet, the magnitude of this fitness cost does not predict the durability of CRISPR-Cas immunity. We contend that this variability in the durability of resistance may be due to variations in phage mutation rate or in the proportion of lethal mutations across the phage genome. These results have important implications for the understanding of the coevolution between bacteria and phages and for the optimal deployment of resistance strategies against pathogens and pests. In a broader perspective, understanding the durability of CRISPR-Cas immunity may also help develop more effective gene-drive strategies based on CRISPR-Cas9 technology.

Introduction

Public health and agriculture are constantly challenged by the spread of infectious diseases. An arsenal of various prophylactic and therapeutic strategies has been developed to limit the circulation of pathogens (e.g. introgression of resistance genes in plant varieties, use of antimicrobial drugs). Yet, the efficacy of those interventions can be rapidly eroded by the evolution of pathogen populations [1, 2, 3, 4]. It is important to note that distinct defense strategies may lead to very different evolutionary outcomes. For instance, imperfect immunity is known to select for more aggressiveness and virulence in pathogens [5, 6]. In addition, distinct defense strategies may differ in their level of *durability*. Why are some host defense strategies overcome very rapidly while others remain effective for a long period of time [4, 7, 8]? A better understanding of the durability of host defenses (defined as the inverse of the speed of pathogen adaptation to those defenses) is key for the development of sustainable management strategies of pathogens and pests [7, 9].

Empirical and experimental studies in plant pathosystems have played key roles in the identification of major factors acting on the durability of host resistance [4, 7, 9, 10, 11]. For instance, the type of plant resistance is known to have a significant impact on the speed of pathogen adaptation. *Qualitative* resistance, an all-or-nothing response, is often considered to be less durable than *quantitative* resistance, which reduces disease progression in the plant. This effect is usually attributed to the simpler genetic determinism of pathogen adaptation to qualitative resistance which involves a few (or even a single) major virulence genes [12]. In contrast, adaptation to the polygenic determinism of quantitative resistance requires multiple pathogen mutations [13, 14]. Yet, qualitative resistance exhibits much variation in durability [4]. A classical explanation for this variation in durability involves selective constraints acting on the pathogen population. More specifically, host defense is likely to be more durable if the mutations (virulence alleles) that allow the pathogen to escape qualitative resistance are associated with fitness costs [4, 12]. Understanding the selective constraints acting on the sites targeted by different resistance mechanisms may help predict the durability of resistance and limit the speed of pathogen adaptation [4, 15]. Testing this hypothesis, however, is often difficult in plant pathosystems where measuring the durability of specific resistance mechanisms in controlled experiments raises practical difficulties [16, 17].

Here we use the interaction between bacteria and their lytic bacteriophages (or phages) to study the factors that modulate the durability of host resistance. Bacteria have access to a wide range of defense systems to defend themselves against phages [18, 19, 20, 21]. Among these distinct defense systems, CRISPR–Cas (Clustered Regularly Interspaced Short Palindromic Repeats – CRISPR Associated Genes) has the unique ability to generate hundreds of different alleles of resistance targeting different sites in the phage genome [22]. Here, we exploit this unique property to explore the variability in durability among distinct CRISPR–Cas resistance alleles targeting the same phage. CRISPR-Cas is an adaptive prokaryotic immune defense which integrates into the CRISPR locus (integration of a spacer) a small phage-DNA sequence (the protospacer, here 30 bp long) from an invading genome and uses this memory to target and degrade subsequent invading matching DNA (interference) [23]. To select and integrate a specific protospacer from a foreign nucleic acid into its CRISPR array, many CRISPR–Cas systems rely on a 2-5 bp sequence, the PAM (Protospacer Adjacent Motif) [24], flanking one side of the protospacer sequence and mandatory for spacer integration and interference. Given its size, the PAM is present numerous times on the phage genome, leading potentially to hundreds of different resistances targeting various protospacers [22]. In this system, phages can only escape CRISPR-Cas by mutating their PAM or seed sequence (ie. the proximal part of the protospacer) [25]. As such, CRISPR-Cas immunity corresponds to a very specific form of *qualitative* resistance. In the following, we first quantified the ability of a phage to escape a set of resistant bacteria, each of them having a distinct new spacer targeting a unique single protospacer site in the phage genome. Second, we isolated escape phage mutants on each of the resistant bacteria (e.g. each phage escape is mutated at a specific and different protospacer region) and we characterized their relative fitness during the infection of a population of phage-sensitive bacteria. This experimental protocol allowed us to discuss the potential link between the fitness effects of escape mutations in the phage and the durability of different resistance alleles in the bacteria.

Materials and Methods

Bacterial strains and phages

The clonal bacterium *Streptococcus thermophilus* DGCC 7710 (WT) and its clonal virulent phage 2972 were obtained from the Félix d'Hérelle Reference Center for Bacterial Viruses (`www.phage.ulaval.ca`) [26]. Bacteria were grown in LM17 broth (M17 Oxoid (37 g/L) with 5g/L of lactose) and incubated at 40°C. For phage amplification 10 mM of sterile $CaCl_2$ were added to the broth. Using a standardized protocol described in [27], a culture

of *S. thermophilus* DGCC 7710 was challenged with the virulent phage 2972, and the surviving colonies/cells (BIMs, Bacteriophage Insensitive Mutants) were screened by PCR for expansion of their CRISPR array, followed by a 2% agarose electrophoresis. Primer sequences and PCR protocol can be found in supplementary information A. We confirmed that each BIM possesses a different spacer by Sanger sequencing the newly acquired spacer (Eurofins Genomics). A total of 17 different BIMs, each with a single and distinct spacer acquired into the active CRISPR1 locus of a type II-A CRISPR-Cas system, were kept and used in this study. Spacer sequences are provided in the supplementary information B. Finally, protospacers were positioned on the genome of phage 2972 that is published in [26].

Phage detection and titration

Bacterial lawns were produced by plating 6 mL of soft agar (LM17+$CaCl_2$ with 0.8% agar and 400 μL of bacteria in mid-exponential phase) on top of plates previously poured with 30 mL of hard agar (LM17+$CaCl_2$ with 1.5% agar). For phage titration, 50 μL of diluted phages were added to soft agar. For phage detection, 5 μL of phage solution were spotted directly on the solidified soft agar. When needed, phages were diluted in phage buffer (50 mM Tris-HCl pH7.5 + 100 mM NaCl + 8 mM $MgSO_4$). Plates were incubated overnight at 40°C and plaques were counted (titration) or recorded (detection).

Durability of resistance

How can we measure the durability of a resistance? The durability of a resistance is defined as the time between its introduction at a large scale and its large circumvention by parasite when conditions are favorable for the parasite development [7]. Consequently, in absence a pre-existing escape parasite, the durability of a resistance depends on two factors: 1) the rate at which escape mutants are generated and 2) their spread into the host population. In the case of an homogeneous resistant host population, any viable escape mutants will inevitably spread quickly into the population. Therefore, in this simple case, the durability of a resistance depends mainly on the rate at which viable escape mutants appears. When escape mutants can only appear by mutation, measuring their rate of apparition is the same as measuring the mutation rate of parasite targeted sequence, here the PAM and seed sequences.

The viable mutation rate of a sequence can be measured using a Luria-Delbrück protocol. The durability of resistance of each of the 17 distincts BIM was measured using a three-steps Luria-Delbrück protocol (see supplemental informations C for a

graphic overview of the protocol). These measurements were replicated 3 times with 3 independent clonal lysates of phage 2972. To ensure that pre-existing escape mutants have not altered these measurements, we measured for each BIM, the initial frequency of escape mutants. The frequency of pre-existing mutants to each of the 17 different BIMs was found to be below 2.9×10^{-5}. Because we inoculated a small quantity of phage 2972 (see below), the impact of the standing genetic variance on the adaptation of the phage was assumed to be negligible.

In the first step of this protocol, for each BIM, WT phages were amplified in 96 independent replicates on the WT-phage-sensitive bacteria (i.e. in the absence of selection). In each replicate, 20 μL of LM17+$CaCl_2$ were inoculated with 0.2 μL of WT bacteria in mid-exponential phase, phages at a concentration of 300 PFU/20μL and incubated at 40°C for 24 hours. We confirmed by titrating four replicates before incubation that $N_i \approx 300$ PFU/20 μL and we measured N_f by titrating 10 randomly chosen lysates. We found $N_f \approx 1.72 \times 10^6$ PFU/20 μL.

In the second step of the protocol, the bacteria from each replicate were pelleted down with a 5-minute centrifugation (6189g) (see supplementary information D) and 25% (5μL) of the supernatant was inoculated into a 200 μL culture of the focal BIM and incubated for 24 hours at 40°C. This second step ensured that even in replicates where the frequency of escape mutants was small at the end of the first step, the frequency of escape mutants would be sufficiently high to be detectable in the third step of the protocol.

In the final and third step of the protocol, the presence of escape phages in each individual replicate was assessed using phage detection assays. P_E, the probability of escape, was calculated as the fraction of replicates where phage escape was detectable. It is possible [28] to estimate the rate of escape mutations against each BIM using:

$$\mu = \frac{-\ln(1 - P_E)}{z(N_f - N_i)}$$

with μ the mutation rate per target sequence (seed and PAM sequences), z the fraction of lysate used for the second amplification (here 1/4), N_f the final number of phages per replicate and N_i the initial number of phages per replicate. To further strenghten the results, the entire protocol has been triplicated with 3 independent clonal phage lysate. Therefore, for each BIM, the estimation of p comes from 288 independant lysates.

Relative fitness of phage escape mutants

For each of the 17 different BIMs, we selected at random 5 phage isolates that escaped bacterial resistance. A single plaque from each of these 5 isolates was amplified in liquid and re-isolated twice on plates, on the BIM on which they were isolated from. After amplification, phages and remaining bacteria were separated by filtration (0.2 μm) and phages were stored in 20% glycerol at -80°C. Genome sequencing (see supplementary information E for the list of primers and F for their protospacer sequence) confirmed that all escape phages contained mutations in their PAM or their seed sequence. This protocol generated a collection of escape mutants for all BIMs.

The relative fitness of all the escape mutants was determined using triplicate competition experiments against a reference phage which contains a 37-bp deletion in its *orf24* (see supplemental information G). This deletion allowed us to readily distinguish the reference strain from all the other escape mutants (see section G in the supplementary information). Approximately 3 000 phages (50% escape mutant and 50% reference phage) were inoculated in 10 mL LM17+$CaCl_2$ supplemented with 100 μL of WT bacteria in early stationary phase. After a 24 hour incubation at 40°C, the remaining bacteria were removed by filtration and phages were stored at -80°C. Before and after amplification, the proportion of the tested phage was measured by qPCR (see section G in the supplementary information). The relative fitness of the escape mutant m was determined using:

$$s_m = r_m - r_{WT} = \log\left(\frac{p_f\,(1-p_i)}{p_i\,(1-p_f)}\right) - \log\left(\frac{p'_f\,(1-p'_i)}{p'_i\left(1-p'_f\right)}\right)$$

where r_m and r_{WT} refer to the malthusian growth rates of the escape mutant and the WT phage, respectively, p_i and p_f (respectively, p'_i and p'_f) are the frequencies of the mutant phage before and after the competition (the prime refers to the frequency of the WT phage 2972).

Statistical analyses

All statistical analyses were run using R Software (version 3.3.2, [29]), through RStudio (Version 1.0.136). For mixed model, R package lme4 version 1.1-13 was used [30].

We performed an Analysis of Variance (ANOVA) to determine if the position of the protospacer on the phage genome impacts the durability of resistances.

Linear models were used for the analysis of relative fitness data. In the first model, we tested the effect of phage genotype on relative fitness. In the second model, we tested the

impact of mutation type (synonymous vs non-synonymous) on relative fitness of phages escaping the BIMs that target an *orf* (36 phage escape mutants). In the third model, we assessed the effect of the relative fitness of phage escape mutants on the durability of resistance of their respective BIM.

Results

To study the durability of various CRISPR alleles, we generated 17 different resistant strains (BIMs) characterized by a new and unique spacer within the CRISPR1 array. Each spacer targets a different protospacer, ie. a different part of the phage genome (supplemental data B). In total, 13 of the 44 phage genes (as well as some non-coding regions) were targeted by at least one spacer, leading to a good coverage of the phage genome by these 17 BIMs (Figure 1).

Our measures of BIMs' durability using fluctuation tests, revealed considerable variation in the ability of the phage to escape different BIMs (Figure 1, supplementary information H, ANOVA, F-value = 10.89, df =16, p-value < 0.001). We also used the probability of escape to estimate the mutation rates for each target sequence (seed and PAM sequences) (see supplementary information I). The average mutation rate was estimated to be 3.4×10^{-7} mutation/target sequence/replication and the escape rate of the less durable BIM was 123 times higher than the one of the most durable BIM.

One possible explanation for the observed variation in durability of resistances is that there are differences in the fitness costs associated with these different escape mutations. Indeed, the Luria-Delbrück protocol used to measure the durability of resistances assume that phage escape mutations are neutral [31]. This assumption is unlikely to be met here and an heterogeneity in the fitness of the escape phage could explain the observed heterogeneity in durability. To explore this hypothesis, we isolated 40 phage mutants escaping the 17 distinct single CRISPR-resistances. A total of 35 escape phages carry a single bp mutation in the targeted sequence, 4 of the remaining phages carry double bp mutations in the targeted sequence, one escape phage has a single bp deletion (see supplementary information F). Among the substitutions, 27 are transversions, 12 are purine transitions and 4 pyrimidine transitions. Ten escape mutants were characterized by synonymous mutations (see supplementary information J).

To measure fitness, we competed each of the escape phage mutants against a reference

phage and measure their relative abondance before and after the experiment. From these data, we deduce relative fitness. We found that relative fitness was highly variable, ranging from -6.21 to 0.68 with an average of -2.22 and a standard deviation of 1.71 (Figure 2, see supplementary information K). Although the majority of the phage escape mutants had a lower fitness than the WT phage (32/40), some escape mutants were neutral (8/40) (Figure 2, supplementary information K). The presence of non-synonymous mutations was not a good predictor of escape mutant fitness (t-value = -0.509, P(R>t) = 0.612) and all tested synonymous mutations but one lower phage fitness (see supplementary information L). Interestingly, we also found that escape mutant fitness was not a good predictor of the durability of each BIM (Figure 3, t-value = -0.423, P(R>t) = 0.673). Hence, the heterogeneity in the durability of CRISPR resistances is not caused by the heterogeneity of fitness costs associated with these escape mutations (see Figure 3).

Discussion

We studied the variation in the ability of the virulent phage 2972 to escape distinct resistance alleles at the CRISPR-Cas immune system of its host *S. thermophilus* DGCC7710. We found i) considerable variation in the durability among these different resistant strains (and therefore in the apparent mutation rate of phage protospacers) and ii) substantial variation in fitness among phages carrying escape mutations. Yet, the cost of those escape mutations was not associated with the durability of their respective resistance strains. If the fitness cost of escape mutations is not a good predictor of resistance durability what drives the variation in durability? We believe that two non-mutually exclusive processes could explain the observed patterns: (i) variation in the mutation rate along the phage genome and (ii) variation in the probability of generating lethal mutations among different sequences targeted by the CRISPR-Cas system.

First, a variation in the mutation rate along the phage genome can result from an heterogeneity of the replication machinery. Such a variation in mutation rates has previously been described in yeast [32], RNA viruses [33] and bacteria [34] but to our knowledge not yet in bacteriophages. The precise mechanism used by phage 2972 to replicate and repair its genome is unknown, limiting our ability to test this hypothesis. However, since phage 2972 encodes and expresses its own replication machinery and does not possess any repair mechanism [26, 35], it is tempting to hypothesize that no repair mechanisms are involved and that the entire replication is made by its replication machinery. This machinery could yield substantial variation among different parts of the phage genome.

Note, however, that most escape mutants we isolated were due to transversions instead of transitions (see supplementary information J), whereas most replication machineries show a biased pattern to transition [32, 36]. If a heterogeneous fidelity rate was at the origin of the observed heterogeneity in durability of resistances, 2972 machinery would have an unconventional mutation bias.

Second, variation in the frequency of lethal mutations along the phage genome could also contribute to the observed variation in BIM durability. Lethal mutations are very common and can reach up to 40% of viruses total mutations [37, 38, 39], but, to our knowledge, the heterogeneity of the probability of lethal mutation along the genome has not been studied. Because some genes are known to be essential while others are accessory (e.g. *orf39* and *orf41* are not expressed during an infection by phage 2972 [35]), we can expect that mutations in different genes should result in different fractions of lethal mutations and, consequently, in variations in the durability among BIMs targeting these different genes.

Additional experiments are required to evaluate the relative importance of the variations in (i) mutation rate and (ii) the proportion of lethals along the phage genome on the durability of CRISPR resistance. The heterogeneity in the mutation rate could be assessed by measuring the durability of several spacers that target different non-functional coding regions of the phage genome. Phage 2972 carry such a sequence in the form of an incomplete lysogeny module that is not expressed [26, 35]. If we could create different BIMs targeting this module, any heterogeneity in durability among those BIMs would only result from an heterogeneity in the mutation rates among the different target sequences. To evaluate the alternative hypothesis that the variation in durability results from variation in the fraction of lethal mutants, one could measure directly this fraction of lethal mutants through the systematic introduction of point mutations in the target sequence of BIMs with contrasted levels of durability [37, 38, 39]. Thanks to recent progress in molecular biology, a range of mutants can be produced by systematically changing each of the nucleotide of the target sequence [40, 41]. The comparison of the number of lethal mutations for a durable and non-durable resistance would allow one to evaluate directly the impact of this factor on the variation of the durability.

CRISPR–Cas immunity is known to generate and maintain a high diversity of resistance alleles against the same phage [22, 42] and this diversity in resistance is known to limit the growth of the phage population [28, 42]. Theoretical models and experimental tests

indicate that such diversity limits the evolutionary emergence of the pathogens [28]. Yet, those studies ignore the heterogeneity in the durability of resistance among different alleles. Our results indicate that another potential benefit of generating this diversity is to explore a range of durability of resistance. The most durable alleles will outcompete the other BIMs and this may provide a very robust way to hamper the evolution of the phage. In addition to this inter-host diversity, a single cell can acquire more than one spacer against the same parasite. The acquisition of multiple spacers targeting different parts of the phage genome implies that the phage needs multiple mutations before it can infect this multiply resistant bacteria [43]. As most escape mutations are costly (Figure 2), carrying multiple escape mutations is likely to reduce dramatically the fitness of the phage. In contrast, the acquisition of multiple spacers does not alter the fitness of the bacteria [44]. This asymmetry may help explaining the ultimate extinction of phage populations coevolving with CRISPR–Cas immunity [22, 45]. It is also important to note that some phages have evolved the ability to defeat CRISPR immunity using anti-CRISPR proteins that inhibit the defense conferred by CRISPR–Cas [46, 47] (note that to our knowledge, phage 2972 does not carry any anti-CRISPR against *S. thermophilus* CRISPR systems). Even though anti-CRISPR can be partially efficient against CRISPR–Cas, the cooperation between phages ensures that, above a minimal concentration, phages can invade a resistant host population without acquiring escape mutations in the sequences targeted by CRISPR–Cas [48, 49].

S. thermophilus is widely used by the dairy industry for the manufacture of several fermented milk products (yoghurt, cheese) and the identification of BIMs with particularly durable resistance could have very practical implications. The use and/or the combination of these BIMs is likely to protect the starter cultures against phage infection. In addition, it would be particularly useful to identify durable spacers that target related phages. Such generalist spacers have been observed before [23]. The use of a durable generalist spacer could massively improve the resistance of *S. thermophilus* strains. Our biological model provides also a unique opportunity to evaluate experimentally the effectiveness of different intervention strategies on the long-term efficacy of resistance to pathogens. It may thus provide important insights for the implementation of sustainable management of pathogens and pests [4, 9, 28].

In addition to these applications in the dairy industry and in agriculture, the CRISPR-Cas9 technology can be used as a driving endonuclease, ie. a genetic tool that make an engineered allele spread into natural populations by non-mendalian heredity [50].

Indeed, in a heterozygote carrying a CRISPR-Cas9 and its guide, the endonuclease will target and cleave the homologous allele. As repair mechanism usually involve homologous DNA sequences, they will usually add a copy of the CRISPR-Cas9 and its guide at the place of the former allele, leading to the rapid spread of the CRISPR-Cas9/guide in the population[50, 51]. However, if the presence of CRISPR-Cas9 is costly for its host, it is likely that escape mutation will emerge and break the spread of the gene-drive [51, 52]. Our results indicate that the durability of gene-drive strategies targeting distinct genome regions is likely to be very variable. Understanding the ultimate source of the variation of durability is particularly important for the effectiveness of gene-drive based on CRISPR-Cas9.

Acknowledgements

The authors thank Alison Feder, Peter Grant, Olivier Tenaillon, Stéphanie Bedhomme, Oliver Kaltz, Elze Hesse, Matthias Grenié and Hélène Pidon for helpful discussions. The authors thank the qPHD, qPCR (head: Philippe Clair) and the GenSeq (head: Frédérique Cerqueira and Erick Desmarais) platforms of the University of Montpellier for their help. E.R.W. further acknowledges the Natural Environment Research Council (`https://nerc.ukri.org`) (NE/M018350/1), the BBSRC (BB/N017412/1), and the European Research Council (`https://erc.europa.eu`) (ERC-STG-2016-714478 - EVOIMMECH) for funding. SM acknowledges funding from the Natural Sciences and Engineering Research Council of Canada (Discovery Program). SM holds the Tier 1 Canada Research Chair in Bacteriophages. HC acknowledges funding from the EMBO (EMBO Short Term Fellowship 7191). SG acknowledges funding from the Leverhulme Trust (Visiting Professorships) and the CNRS (PEPS MPI grant).

References

[1] O'Neill (chair) J. Tackling drug-resistant infections globally: final report and recommendations. The review on antimicrobial resistance. Commissioned by the UK Prime Minister. 2016;Available from: `http://amr-review.org/Publications`.

[2] Feder AF, Rhee SY, Holmes SP, Shafer RW, Petrov DA, Pennings PS. More effective drugs lead to harder selective sweeps in the evolution of drug resistance in HIV-1. eLife. 2016 feb;5:e10670. Available from: `https://doi.org/10.7554/eLife.10670`.

[3] Ghany MG, Doo EC. Antiviral resistance and hepatitis B therapy. Hepatology. 2009;49(S5):S174–S184. Available from: `http://dx.doi.org/10.1002/hep.22900`.

[4] Leach JE, Cruz CMV, Bai J, Leung H. Pathogen fitness penalty as a predictor of durability of disease resistance genes. Annual Review of Phytopathology. 2001;39(1):187–224. Available from: https://doi.org/10.1146/annurev.phyto.39.1.187.

[5] Gandon S, Michalakis Y. Evolution of parasite virulence against qualitative or quantitative host resistance. Proceedings of the Royal Society of London B: Biological Sciences. 2000;267(1447):985–990. Available from: http://rspb.royalsocietypublishing.org/content/267/1447/985.

[6] Gandon S, Mackinnon MJ, Nee S, Read AF. Imperfect vaccines and the evolution of pathogen virulence. Nature. 2001 12;414:751. Available from: https://www.nature.com/articles/414751a.

[7] Johnson R. A critical analysis of durable resistance. Annual Review of Phytopathology. 1984;22(1):309–330. Available from: https://doi.org/10.1146/annurev.py.22.090184.001521.

[8] Kennedy DA, Read AF. Why does drug resistance readily evolve but vaccine resistance does not? Proceedings of the Royal Society of London B: Biological Sciences. 2017;284(1851). Available from: http://rspb.royalsocietypublishing.org/content/284/1851/20162562.

[9] Mundt CC. Durable resistance: A key to sustainable management of pathogens and pests. Infection, Genetics and Evolution. 2014;27:446 – 455. Available from: http://www.sciencedirect.com/science/article/pii/S1567134814000148.

[10] Johnson R. Durable resistances: definition of, genetic control, and attainment in plant breeding. Phytopathology. 1981;71(6):567–568. Available from: https://www.apsnet.org/publications/phytopathology/backissues/Documents/1981Articles/Phyto71n06_567.PDF.

[11] McDonald BA, Linde C. Pathogen population genetics, evolutionary potential, and durable resistance. Annual Review of Phytopathology. 2002;40(1):349–379. Available from: https://doi.org/10.1146/annurev.phyto.40.120501.101443.

[12] Flor HH. Current status of the gene-for-gene concept. Annual Review of Phytopathology. 1971;9(1):275–296. Available from: https://doi.org/10.1146/annurev.py.09.090171.001423.

[13] Stuthman DD, Leonard KJ, Miller-Garvin J. Breeding crops for durable resistance to disease. vol. 95 of Advances in Agronomy. Academic Press; 2007. p. 319 – 367. Available from: http://www.sciencedirect.com/science/article/pii/S006521130795004X.

[14] Poland JA, Balint-Kurti PJ, Wisser RJ, Pratt RC, Nelson RJ. Shades of gray: the world of quantitative disease resistance. Trends in Plant Science. 2009 2018/09/02;14(1):21–29. Available from: https://www.sciencedirect.com/science/article/pii/S1360138508002975.

[15] Lafforgue G, Martínez F, Niu QW, Chua NH, Daròs JA, Elena SF. Improving the effectiveness of artificial microRNA (amiR)-mediated resistance against Turnip Mosaic Virus by combining two amiRs or by targeting highly conserved viral genomic regions. Journal of Virology. 2013;87(14):8254–8256. Available from: http://jvi.asm.org/content/87/14/8254.abstract.

[16] Kousik CS, Ritchie DF. Development of bacterial spot on near-isogenic lines of bell pepper carrying gene pyramids composed of defeated major resistance genes. Phytopathology. 1999 2018/07/03;89(11):1066–1072. Available from: https://doi.org/10.1094/PHYTO.1999.89.11.1066.

[17] Brun H, Levivier S, Somda I, Ruer D, Renard M, Chèvre AM. A field method for evaluating the potential durability of new resistance sources: application to the *Leptosphaeria maculans-Brassica napus* pathosystem. Phytopathology. 2000 2018/07/03;90(9):961–966. Available from: https://doi.org/10.1094/PHYTO.2000.90.9.961.

[18] Labrie SJ, Samson JE, Moineau S. Bacteriophage resistance mechanisms. Nat Rev Micro. 2010 03;8(5):317–327. Available from: https://www.nature.com/articles/nrmicro2315.

[19] Goldfarb T, Sberro H, Weinstock E, Cohen O, Doron S, Charpak-Amikam Y, et al. BREX is a novel phage resistance system widespread in microbial genomes. The EMBO Journal. 2015;34(2):169–183. Available from: http://emboj.embopress.org/content/34/2/169.

[20] Ofir G, Melamed S, Sberro H, Mukamel Z, Silverman S, Yaakov G, et al. DISARM is a widespread bacterial defence system with broad anti-phage activities. Nature Microbiology. 2018;3(1):90–98. Available from: https://www.nature.com/articles/s41564-017-0051-0.

[21] Doron S, Melamed S, Ofir G, Leavitt A, Lopatina A, Keren M, et al. Systematic discovery of antiphage defense systems in the microbial pangenome. Science. 2018;359(6379). Available from: http://science.sciencemag.org/content/359/6379/eaar4120.

[22] Paez-Espino D, Morovic W, Sun CL, Thomas BC, Ueda Ki, Stahl B, et al. Strong bias in the bacterial CRISPR elements that confer immunity to phage. Nature Communications. 2013;4:1430. Available from: https://www.nature.com/articles/ncomms2440.

[23] Barrangou R, Fremaux C, Deveau H, Richards M, Boyaval P, Moineau S, et al. CRISPR provides acquired resistance against viruses in prokaryotes. Science. 2007;315(5819):1709. Available from: http://science.sciencemag.org/content/315/5819/1709.

[24] Horvath P, Romero DA, Coûté-Monvoisin AC, Richards M, Deveau H, Moineau S, et al. Diversity, activity, and evolution of CRISPR loci in *Streptococcus thermophilus*. Journal of Bacteriology. 2008 02;190(4):1401–1412. Available from: https://onlinelibrary.wiley.com/doi/abs/10.1111/j.1462-2920.2012.02879.x.

[25] Sun CL, Barrangou R, Thomas BC, Horvath P, Fremaux C, Banfield JF. Phage mutations in response to CRISPR diversification in a bacterial population. Environmental Microbiology. 2013;15(2):463–470. Available from: https://onlinelibrary.wiley.com/doi/abs/10.1111/j.1462-2920.2012.02879.x.

[26] Lévesque C, Duplessis M, Labonté J, Labrie S, Fremaux C, Tremblay D, et al. Genomic organization and molecular analysis of virulent bacteriophage 2972 infecting an exopolysaccharide-producing *Streptococcus thermophilus* strain. Applied and Environmental Microbiology. 2005 07;71(7):4057–4068. Available from: https://aem.asm.org/content/71/7/4057.

[27] Hynes AP, Lemay ML, Trudel L, Deveau H, Frenette M, Tremblay DM, et al. Detecting natural adaptation of the *Streptococcus thermophilus* CRISPR-Cas systems in research and classroom settings. Nature Protocols. 2017 02;12:547. Available from: http://dx.doi.org/10.1038/nprot.2016.186.

[28] Chabas H, Lion S, Nicot A, Meaden S, van Houte S, Moineau S, et al. Evolutionary emergence of infectious diseases in heterogeneous host populations. PLOS Biology. 2018 09;16(9):1–20. Available from: https://doi.org/10.1371/journal.pbio.2006738.

[29] R Core Team. R: A language and environment for statistical computing. Vienna, Austria; 2016. Available from: https://www.R-project.org/.

[30] Bates D, Mächler M, Bolker B, Walker S. Fitting linear mixed-effects models using lme4. Journal of Statistical Software. 2015;67(1):1–48. Available from: https://www.jstatsoft.org/article/view/v067i01.

[31] Luria SE, Delbrück M. Mutations of bacteria from virus sensitiviy to virus resistance. Genetics. 1943;28(6):491–511. Available from: http://www.genetics.org/content/28/6/491.

[32] Lujan SA, Clausen AR, Clark AB, MacAlpine HK, MacAlpine DM, Malc EP, et al. Heterogeneous polymerase fidelity and mismatch repair bias genome variation and composition. Genome Research. 2014;24(11):1751–1764. Available from: http://genome.cshlp.org/content/24/11/1751.abstract.

[33] Geller R, Estada Ú, Peris JB, Andreu I, Bou JV, Garijo R, et al. Highly heterogeneous mutation rates in the hepatitis C virus genome. Nature Microbiology. 2016 04;1:16045 EP –. Available from: http://dx.doi.org/10.1038/nmicrobiol.2016.45.

[34] Dillon MM, Sung W, Lynch M, Cooper VS. Periodic Variation of Mutation Rates in Bacterial Genomes Associated with Replication Timing. mBio. 2018;9(4). Available from: https://mbio.asm.org/content/9/4/e01371-18.

[35] Young JC, Dill BD, Pan C, Hettich RL, Banfield JF, Shah M, et al. Phage-induced expression of CRISPR-associated proteins is revealed by shotgun proteomics in *Streptococcus thermophilus*. PLOS ONE. 2012 05;7(5):1–12. Available from: https://doi.org/10.1371/journal.pone.0038077.

[36] Hestand MS, Houdt JV, Cristofoli F, Vermeesch JR. Polymerase specific error rates and profiles identified by single molecule sequencing. Mutation Research/Fundamental and Molecular Mechanisms of Mutagenesis. 2016;784-785:39 – 45. Available from: http://www.sciencedirect.com/science/article/pii/S0027510716300045.

[37] Sanjuán R, Moya A, Elena SF. The distribution of fitness effects caused by single-nucleotide substitutions in an RNA virus. Proceedings of the National Academy of Sciences. 2004;101(22):8396–8401. Available from: http://www.pnas.org/content/101/22/8396.

[38] Domingo-Calap P, Cuevas JM, Sanjuán R. The fitness effects of random mutations in single-stranded DNA and RNA bacteriophages. PLOS Genetics. 2009;5(11):1–7. Available from: https://doi.org/10.1371/journal.pgen.1000742.

[39] Peris JB, Davis P, Cuevas JM, Nebot MR, Sanjuán R. Distribution of fitness effects caused by single-nucleotide substitutions in bacteriophage f1. Genetics. 2010;185(2):603–609. Available from: http://www.genetics.org/content/185/2/603.

[40] Martel B, Moineau S. CRISPR-Cas: an efficient tool for genome engineering of virulent bacteriophages. Nucleic Acids Research. 2014;42(14):9504–9513. Available from: http://dx.doi.org/10.1093/nar/gku628.

[41] Lemay ML, Tremblay DM, Moineau S. Genome engineering of virulent lactococcal phages using CRISPR-Cas9. ACS Synthetic Biology. 2017;6(7):1351–1358. Available from: https://doi.org/10.1021/acssynbio.6b00388.

[42] van Houte S, Ekroth AKE, Broniewski JM, Chabas H, Ashby B, Bondy-Denomy J, et al. The diversity-generating benefits of a prokaryotic adaptive immune system. Nature. 2016 04;532:385. Available from: http://dx.doi.org/10.1038/nature17436.

[43] Deveau H, Barrangou R, Garneau JE, Labonté J, Fremaux C, Boyaval P, et al. Phage response to CRISPR-encoded resistance in *Streptococcus thermophilus*. Journal of Bacteriology. 2008;190(4):1390–1400. Available from: http://jb.asm.org/content/190/4/1390.abstract.

[44] Vale PF, Lafforgue G, Gatchitch F, Gardan R, Moineau S, Gandon S. Costs of CRISPR-Cas-mediated resistance in *Streptococcus thermophilus*. Proceedings of the Royal Society of London B: Biological Sciences. 2015;282(1812). Available from: http://rspb.royalsocietypublishing.org/content/282/1812/20151270.

[45] Weissman JL, Holmes R, Barrangou R, Moineau S, Fagan WF, Levin B, et al. Immune loss as a driver of coexistence during host-phage coevolution. The Isme Journal. 2018 01;12:585 EP –. Available from: http://dx.doi.org/10.1038/ismej.2017.194.

[46] Bondy-Denomy J, Pawluk A, Maxwell KL, Davidson AR. Bacteriophage genes that inactivate the CRISPR/Cas bacterial immune system. Nature. 2012 12;493:429. Available from: http://dx.doi.org/10.1038/nature11723.

[47] Hynes AP, Rousseau GM, Agudelo D, Goulet A, Amigues B, Loehr J, et al. Widespread anti-CRISPR proteins in virulent bacteriophages inhibit a range of Cas9 proteins. Nature Communications. 2018;9(1):2919. Available from: https://doi.org/10.1038/s41467-018-05092-w.

[48] Landsberger M, Gandon S, Meaden S, Rollie C, Chevallereau A, Chabas H, et al. Anti-CRISPR phages cooperate to overcome CRISPR-Cas immunity. Cell. 2018 2018/08/30;174(4):908–916.e12. Available from: https://doi.org/10.1016/j.cell.2018.05.058.

[49] Borges AL, Zhang JY, Rollins MF, Osuna BA, Wiedenheft B, Bondy-Denomy J. Bacteriophage cooperation suppresses CRISPR-Cas3 and Cas9 immunity. Cell. 2018 2018/08/30;174(4):917–925.e10. Available from: https://doi.org/10.1016/j.cell.2018.06.013.

[50] Godfray HCJ, North A, Burt A. How driving endonuclease genes can be used to combat pests and disease vectors. BMC Biology. 2017 Sep;15(1):81. Available from: https://doi.org/10.1186/s12915-017-0420-4.

[51] Noble C, Adlam B, Church GM, Esvelt KM, Nowak MA. Current CRISPR gene drive systems are likely to be highly invasive in wild populations. eLife. 2018 jun;7:e33423. Available from: https://doi.org/10.7554/eLife.33423.

[52] Unckless RL, Clark AG, Messer PW. Evolution of resistance against CRISPR/Cas9 gene drive. Genetics. 2017;205(2):827–841. Available from: http://www.genetics.org/content/205/2/827.

Figures & Legends

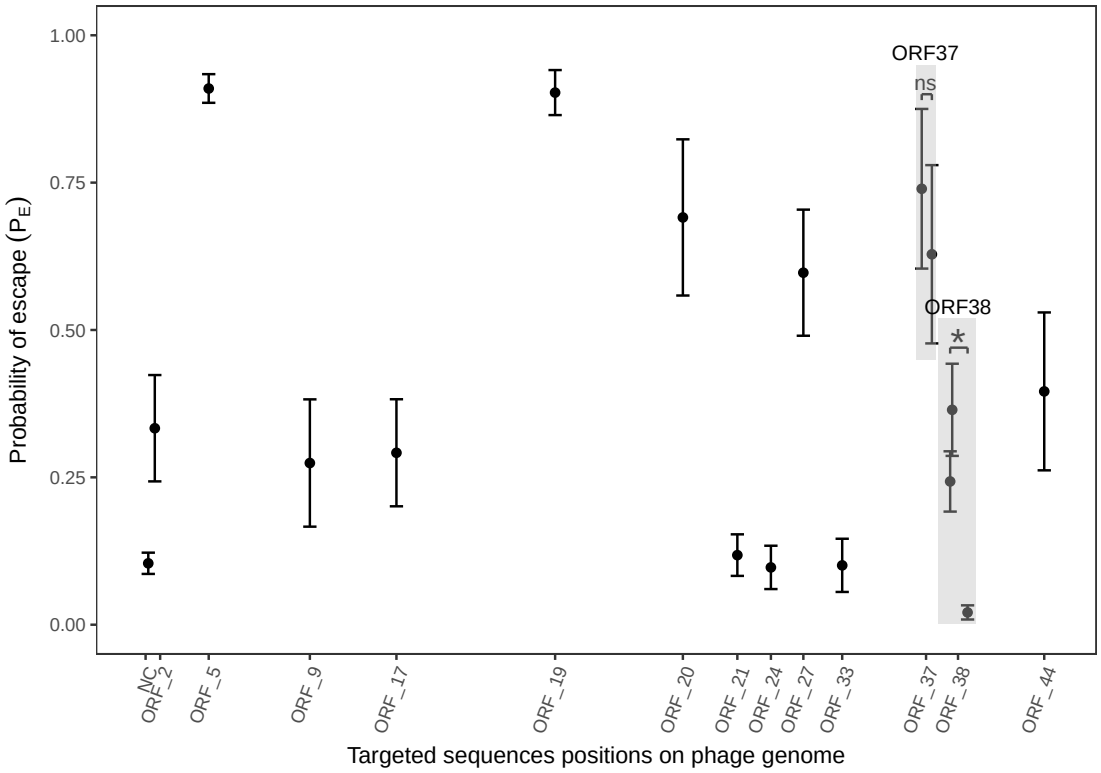

Figure 1: **Variability in the durability of CRISPR–Cas immunity.**
The mutation rate of 17 protospacers whose positions are labelled on the x-axis were measured using fluctuation tests. P_E values, ie. the number of replicates in which a phage escape mutant evolved, are reported and show heterogeneity among the targeted sequences, implying that there is heterogeneity in the durability of CRISPR–Cas resistances. The two protospacers of *orf*37 have the same mutation rate but at least one of the protospacer of *orf*38 has a lower mutation rate.

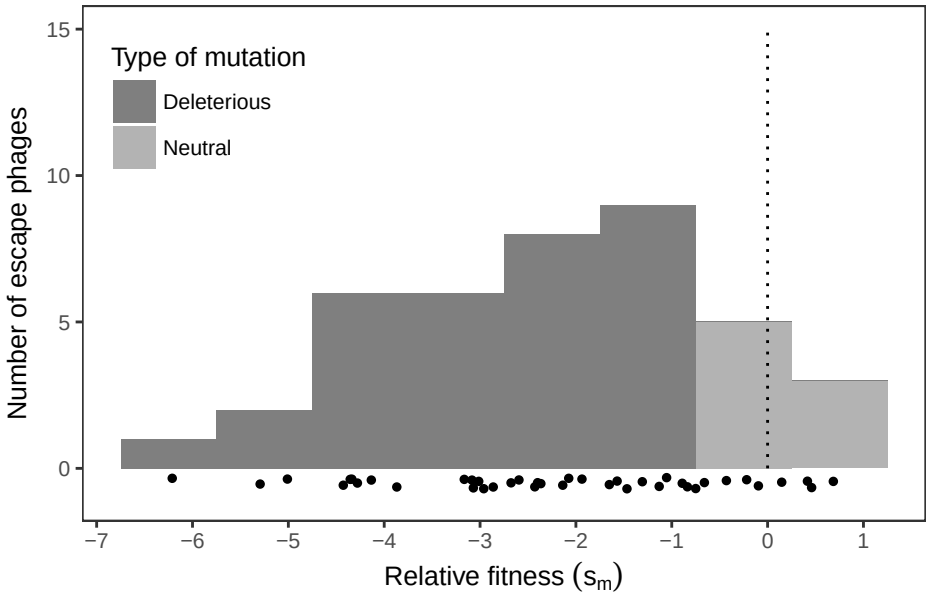

Figure 2: **Distribution of fitness effects of escape mutations in the phage.** Relative fitness was measured through competition experiments with a collection of 40 escape phages, mutated on their seed or PAM sequences. Phages that carry a neutral and deleterious mutations are represented in medium and dark grey respectively. Black dots show the relative fitness of each escape phage. The dotted segment represents the fitness of WT phage 2972. Fitness value of each escape phage is also provided in the supplementary informations K.

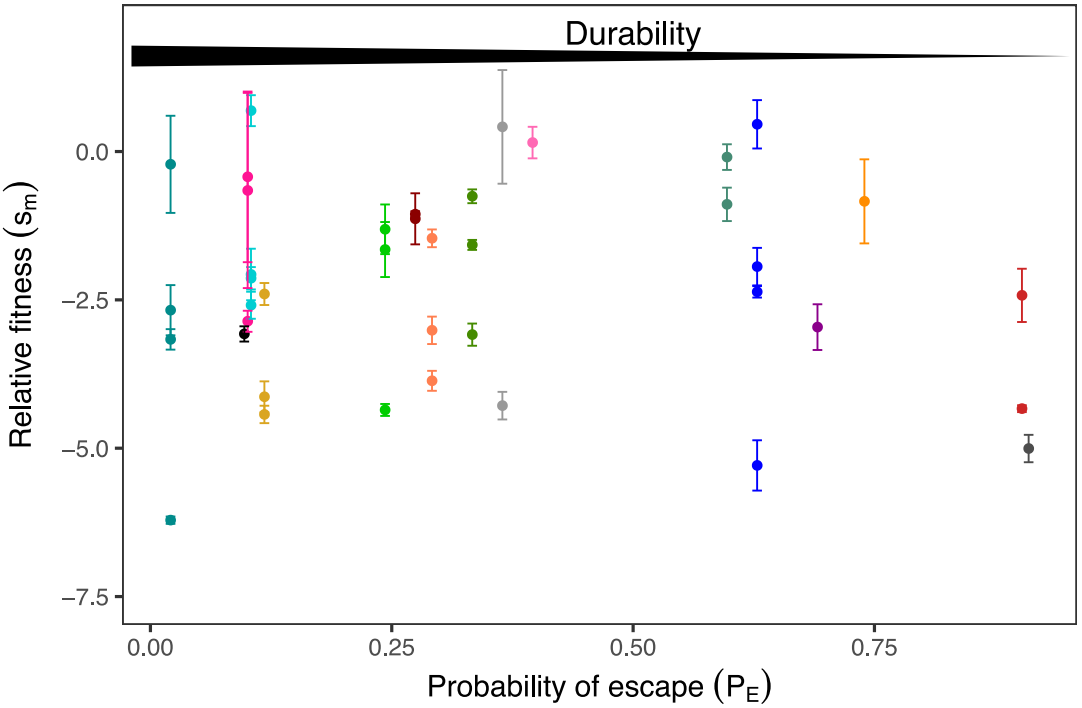

Figure 3: **Relative fitness of phage escape mutants against durability (probability of escape P_E) of their respective BIM.**
Each color corresponds to a single BIM and each dot to a single escape phage. Error bars correspond to 95% Confidence Intervals. Raw data are provided in supplementary informations I and K.

Supplementary informations

A. Primers used for CRISPR PCR and sequencing

A.1. PCR Protocol

The PCR mix contained 5 μL of Multiplex Qiagen, 1 μL of each primer, 2 μL of sterile water and 1 μL of 1% bacteria. The PCR program involves 15 minutes at 94°C, 35 cycles of 30 seconds at 94°C, 90 seconds at 60°C (CRISPR1 and 2) or 56°C (CRISPR3 and 4), 1 minute at 72°C and ended by 10 minutes at 60°C.

A.2. Primers

Table S1: Primer sequences used for the PCR of *S. thermophilus* loci.

CRISPR	Forward Primer (5'-3')	Reverse primer (5'-3')
1	TGCTGAGACAACCTAGTCTCTC	GGATCCGGATCCGTTGAGGCCTTGTTC
2	GCCCCTACCATAGTGCTGAAAAATTAG	CCAAATCTTGTGCAGGATGGTCG
3	GGTGACAGTCACATCTTGTCTAAAACG	GCTGGATATTCGTATAACATGTC
4	CCTCATAGAGCTTTGAAAGATGCTAGAC	GTTCTTCTTGATGCTTGTCGAGGC

B. Characterization of BIMs

Table S2: BIMs spacer sequence and protospacer position in 2972 phage genome. BIMs are named with the following nomenclature: NC or ORF indicates if the BIM targets a non-coding or a coding sequence respectively. When appropriate, the number following the _ sign indicates the targeted *orf*. If multiple BIMs target the same *orf*, they are distinguished by capital letters.

Name	Spacer sequence (5'-3')	Protospacer position in the phage genome	*orf* targeted in the phage genome
NC	AGGAGGTGGACATATTGGGCTAAATCAACG	954 – 983	non-coding
ORF_2	GCTCTACGACTTCTTCCACGAGTTCCTGCC	1 199 – 1 228	2
ORF_5	CCATCTCGTTGTCCTTACGACGACCAGACT	3 223 – 3 252	5
ORF_9	AGATATTGATTATGGTGTTAAAGCAGACCA	7 020 – 7 049	9
ORF_17	AAGCAAGTTGATATATTTCTCTTTCTTTAT	10 270 – 10 299	17
ORF_19	TTATCTGATTTTTTCCCCTTGATTTCGGGG	16 226 – 16 255	19
ORF_20	TAAGGCAAACGAGACCGAGAGAGCTGCAGC	21 022 – 21 051	20
ORF_21	TTGACGATTGGGAACCGTGGAAGGAATTTG	23 067 – 23 096	21
ORF_24	AACACAGATGTTTTAGACCATGCGCAGAAG	24 326 – 24 355	24 + non-coding
ORF_27	TATTTGTACGTGAGTGGAAGTGCTTAGACT	25 544 – 25 473	27 + non-coding
ORF_33	TTTCATCGTCAATTTCCATGTTATAAATCT	27 003 – 27 032	33
ORF_37_A	TCGTTTTCAGTCATTGGTGGTTTGTCAGCG	29 988 – 30 017	37

Continued on next page.

Name	Spacer sequence (5'-3')	Protospacer position in the phage genome	*orf* targeted in the phage genome
ORF_37_B	AGAAGCACCTCTTGCGTTGATAAAAGTATT	30 369 – 30 398	37
ORF_38_A	ATATTCATATTCCCTGCTCATGTTTGATAG	31 055 – 31 084	38
ORF_38_B	CTTTATACTCGTTAAGAATGGCATCTACGA	31 132 – 31 161	38
ORF_38_C	CACATATCGACGTATCGTGATTATCCCATT	31 709 – 31 737	38
ORF_44	AGCCTAGATAGCGAAGTTGATCGTATCTAT	34 587 – 34 616	44

530

C. Graphic overview of Luria-Delbrück protocol

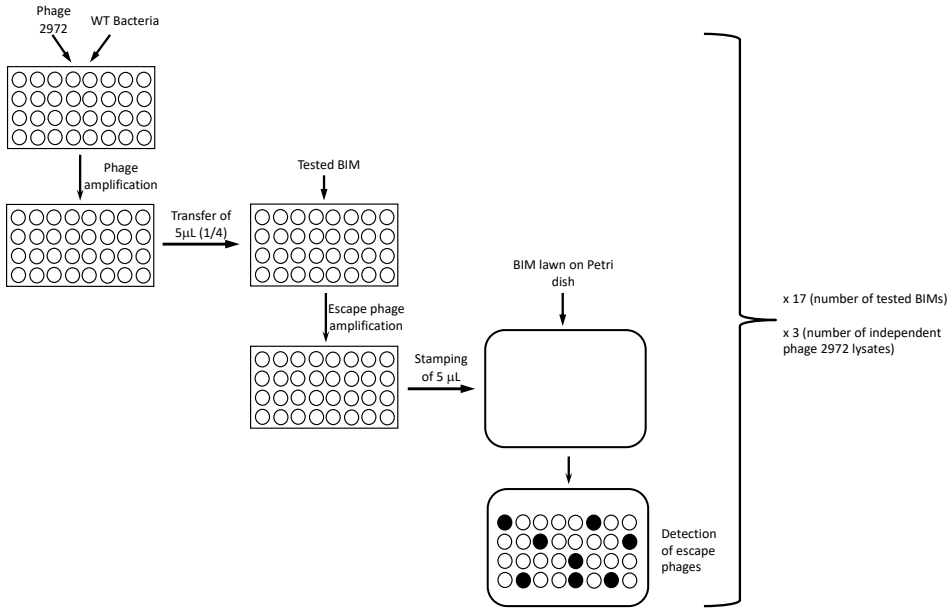

D. Impact of centrifugation on phage titre in lysate

Table S3: **Impact of centrifugation on phage titre. Centrifugation does not modify phage titre.**

Titre before centrifugation (PFU/mL)	Titre after centrifugation (PFU/mL)
8.2×10^8	5.6×10^8
1.0×10^9	7.8×10^8
1.2×10^9	6.6×10^8
9.2×10^8	9.2×10^8

W=14.5, p-value=0.081 : No statistical differences in phage titer before and after centrifugation.

E. Primers used for escape phages sequencing

Table S4: **Primers used for sequencing escape phages.**
Phages are named with the following nomenclature: 2972 indicates that it is a phage derived from 2972 phage; NC or ORF indicates whether the protospacer is part of a non-coding or a coding sequence respectively. When appropriate, the number following the _ sign indicates the *orf* in which the protospacer is located. If a given *orf* contains several protospacers, they are distinguished by a capital letter.

Phage	Left Primer	Right Primer
2972_NC	TAGCGGAATTTTCACGGTCT	CCTGTAGCGGCATTTAGCTC
2972_ORF_2	CTTGCTTAGCCGTTGGGTAG	GGCTCATTTGTGGGTTGTCT
2972_ORF_5	CGGATAGGATTGCCAGCTAA	GTCATCGGTAGCACAGAGCA
2972_ORF_9	AAAACGACCGTCAACAGCTT	GTAGATGCAGCCTTGCGAAT
2972_ORF_17	AGAGCGCTAGACATGCCATT	AGAGGCGACCGAGTAAGTGA
2972_ORF_19	TCAGAGCCTTGCACAACATC	GCGGCACTTTCTTGTATGGT
2972_ORF_20	AGAGATGGAAGCCAAAGCAA	AAGATCCCGTTCTCGATGTG
2972_ORF_21	ATGGAAAGCCTAGCGTTGAA	TGTGGCTAGCTCCTTCGTTT
2972_ORF_24	TCGGATTGCTACCGAAAATC	CAATCTGCTCCACTGCGTTA
2972_ORF_27	AATACCGTGCCAAGTCTGGT	GGGATCCCATTTTCTCATTACT
2972_ORF_33	AATGTCTGCCTCAAGCGACT	GTGTGCGGAGTGCAACTAAA
2972_ORF_37_A	CTTGCATGTTCCCAATTCCT	ACCGATATCCCACTTCCAGA
2972_ORF_37_B	AAGGAATTGGGAACATGCAA	ACTCGGCTAGGGCGTTATTT
2972_ORF_38_A	TCCCATCCGTTTATGGTAGG	ACCCTCGAAAATGGGAAAGT
2972_ORF_38_B	ACCCTCGAAAATGGGAAAGT	TCCCATCCGTTTATGGTAGG
2972_ORF_38_C	TTGCCATTATCGAAGGGAAG	CGAGTGGAAACGACATCTGA
2972_ORF_44	TCGCAAGGAAATCCAAGAGT	CGTTTAACACTTTCCTTTTCAAGA

F. Sequences of escape phages protospacer

Table S5: Sequences of escape phages protospacer and PAM. Mutations are highlighted in grey and their PAM is framed. WT and lower case letters indicate if the sequence corresponds to the WT phage 2972 or an escape mutant.

Phage escape mutants	Protospacer + PAM
2972_NC_WT	AGGAGGTGGACATATTGGGCTAAATCAACGAC AGAA
2972_NC_a	AGGAGGTGGACATATTGGGCTAAATCGACGAC AGAA
2972_NC_c	AGGAGGTGGACATATTGGGCTAAATCAACGAC AGAG
2972_NC_d	AGGAGGTGGACATATTGGGCTAAACCAACGAC AGAA
2972_NC_e	AGGAGGTGGACATATTGGGCTAAATCACCGAC AGAA
2972_ORF_2_WT	GCTCTACGACTTCTTCCACGAGTTCCTGCCTC AGAA
2972_ORF_2_a	GCTCTACGACTTCTTCCACGAGTTCCTGCCTC ATAA
2972_ORF_2_b	GCTCTACGACTTCTTCCACGAGTTCCTGCCTC AAAA
2972_ORF_2_c	GCTCTACGACTTCTTCCACGAGTTCCTTCCTC AGAA
2972_ORF_5_WT	CCATCTCGTTGTCCTTACGACGACCAGACTTG AGAA
2972_ORF_5_a	CCATCTCGTTGTCCTTACGACGACCATACTTG AGAA
2972_ORF_9_WT	AGATATTGATTATGGTGTTAAAGCAGACCATA AGAA
2972_ORF_9_a	AGATATTGATTATGGTGTTAAAGCAGAGCATA AGAA
2972_ORF_9_b	AGATATTGATTATGGTGTTAAAGCAGAAAATA AGAA
2972_ORF_17_WT	AAGCAAGTTGATATATTTCTCTTTCTTTATTA AGAA
2972_ORF_17_a	AAGCAAGTTGATATATTTCTCTTTCTTTATTA AGAG
2972_ORF_17_b	AAGCAAGTTGATATATTTCTCTTTCTTTGTTA AGAA
2972_ORF_17_d	AAGCAAGTTGATATATTTCTCTTTCTTTATTA ATAA
2972_ORF_19_WT	TTATCTGATTTTTTCCCCTTGATTTCGGGGAT AGAA
2972_ORF_19_a	TTATCTGATTTTTTCCCCTTGATTTCGCGGAT AGAA
2972_ORF_19_b	TTATCTGATTTTTTCCCCTTGATTTCTTGGAT AGAA
2972_ORF_20_WT	TAAGGCAAACGAGACCGAGAGAGCTGCAGCCG AGAA
2972_ORF_20_b	TAAGGCAAACGAGACCGAGAGAGCTGCAGCCG AGAC
2972_ORF_21_WT	TTGACGATTGGGAACCGTGGAAGGAATTTGCA AGAA
2972_ORF_21_a	TTGACGATTGGGAACCGTGGAAGGAATTTGCA AGAC
2972_ORF_21_c	TTGACGATTGGGAACCGTGGAAGGAATTTGCA AGTA
2972_ORF_21_d	TTGACGATTGGGAACCGTGGAAGGAATTTGCA AAAA

Continued on next page.

Phage escape mutants	Protospacer + PAM
2972_ORF_24_WT	AACACAGATGTTTTAGACCATGCGCAGAAGGGAGAA
2972_ORF_24_c	AACACAGATGTTTTAGACCATGCGCAGA-GGGAGAA
2972_ORF_27_WT	TATTTGTACGTGAGTGGAAGTGCTTAGACTTTAGAA
2972_ORF_27_a	TATTTGTACGTGAGTGGAAGTGCTTAGACTTTAAAA
2972_ORF_27_d	TATTTGTACGTGAGTGGAAGTGCTTAGTCTTTAGAA
2972_ORF_33_WT	TTTCATCGTCAATTTCCATGTTATAAATCTCTAGAA
2972_ORF_33_a	TTTCATCGTCAATTTCCATGTTATAAATCTCTAAAA
2972_ORF_33_b	TTTCATCGTCAATTTCCATGTTATAAATCTCTTGAA
2972_ORF_33_c	TTTCATCGTCAATTTCCATGTTATAAATTTCTAAAA
2972_ORF_37_A_WT	TCGTTTTCAGTCATTGGTGGTTTGTCAGCGAAAGAA
2972_ORF_37_A_a	TCGTTTTCAGTCATTGGTGGTTTGTCAGCGAAAGAG
2972_ORF_37_B_WT	AGAAGCACCTCTTGCGTTGATAAAAGTATTGCAGAA
2972_ORF_37_B_a	AGAAGCACCTCTTGCGTTGATAAAAGTTTTGCAGAA
2972_ORF_37_B_b	AGAAGCACCTCTTGCGTTGATAAAAGCATTGCAGAA
2972_ORF_37_B_c	AGAAGCACCTCTTGCGTTGATAAAAGTATTGCAAAA
2972_ORF_37_B_d	AGAAGCACCTCTTGCGTTGATAAAATTATTGCAGAA
2972_ORF_38_A_WT	ATATTCATATTCCCTGCTCATGTTTGATAGCAAGAA
2972_ORF_38_A_a	ATATTCATATTCCCTGCTCATGTTTGAAAGCAAGAA
2972_ORF_38_A_b	ATATTCATATTCCCTGCTCATGTTTGTTAGCAAGAA
2972_ORF_38_A_e	ATATTCATATTCCCTGCTCATGTTCGATAGCAAGAA
2972_ORF_38_B_WT	CTTTATACTCGTTAAGAATGGCATCTACGACAAGAA
2972_ORF_38_B_a	CTTTATACTCGTTAAGAATGGCATCTTCGACAAGAA
2972_ORF_38_B_c	CTTTATACTCGTTAAGAATGGCATCTACGACAATAA
2972_ORF_38_C_WT	ACATATCGACGTATCGTGATTATCCCATTCAAGAA
2972_ORF_38_C_a	ACATATCGACGTATCGTGATTATACAATTCAAGAA
2972_ORF_38_C_b	ACATATCGACGTATCGTGATTATCCCATTCATGAA
2972_ORF_38_C_c	ACATATCGACGTATCGTGATTATCCCCTTCAAGAA
2972_ORF_38_C_e	ACATATCGACGTATCGTGATTATGCCATTCAAGAA
2972_ORF_44_WT	AGCCTAGATAGCGAAGTTGATCGTATCTATTTAGAA
2972_ORF_44_b	AGCCTAGATAGCGAAGTTGATCGTATCTGTTTAGAA

538

G. Measure of phages fitness: determination of phage proportion during the competition experiment

The qPCR mix was composed of 3 μL of 2X Master Mix, 0.3 μL of primers at 10 μM, 1.7 μl of water and 1 μl of phages solution at 10^5 or 10^6 PFU/mL. To specifically target the referee phage (ie the phage with a 37-bp deletion), we used primers 5'-TAGACCATGCGCAGAAGGGA–3' and 5'-CCACGATTTCAACGATACGC-3'. To amplify all phages, we used 5'-GAAAATCAGCAGCAAATGGC-3' and 5'-TGACCA-CATCTTCTAAGCCGT-3'. The qPCR program was as follows: an initial denaturation at 95°C for 10 minutes, 45 amplification cycles of 15 seconds at 95°C, 20 seconds at 58°C, 25 seconds at 72°C. To obtain melting curves, temperature reached 95°C for 5 seconds, 60°C for a minute and rose to 97°C at a rate of 0.11°C per second. The DNA was cooled down at 40°C for 30 seconds. Calibration curve was obtained by applying this protocol to known-phage ten-times dilutions from 10^7 PFU/mL to 10^3 PFU/mL. To attribute an absolute number of phages to each qPCR point, these dilutions were titrated simultaneously (see above).

In our collection, the Reference phage is targeted by the BIM that target *orf24* and carries a 37 bp deletion in its protospacer.

H. Durability of CRISPR resistances

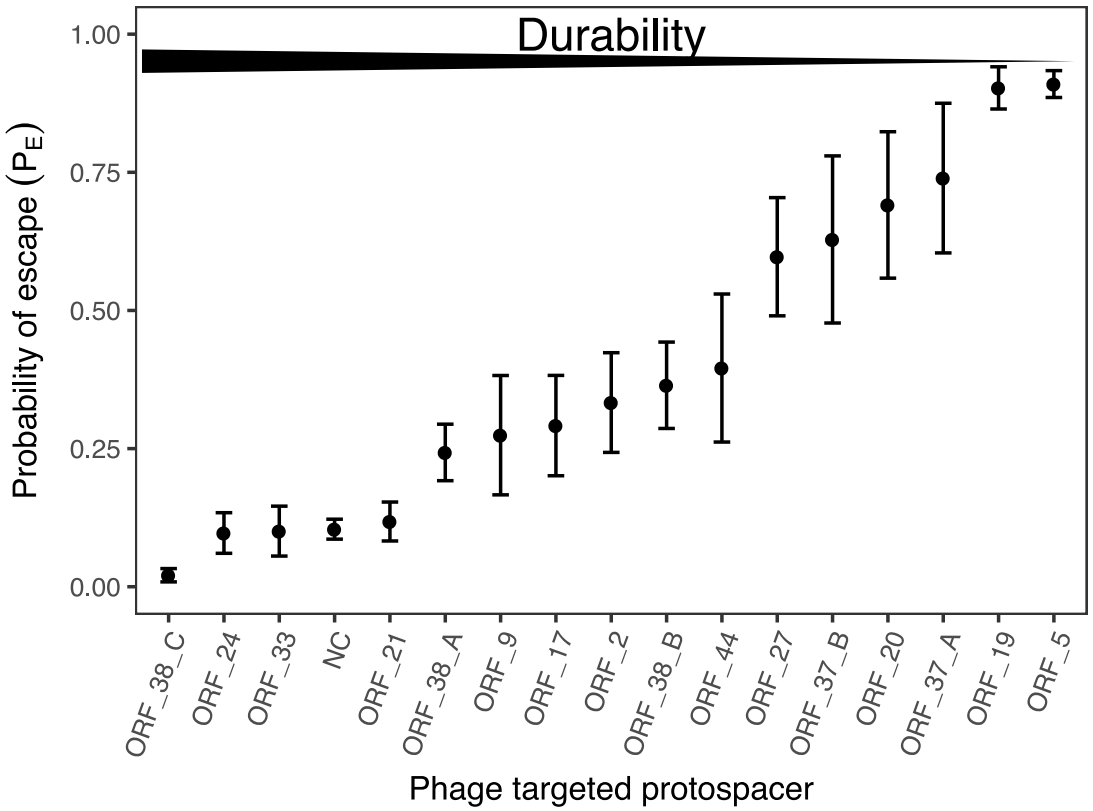

Figure S1: **Variability in the durability of CRISPR–Cas immunity.** The probability of escape P_E was measured for each BIM using fluctuation tests. Mutation rates of each protospacer can be found in supplementary information I.

I. Mutation rate of CRISPR-targeted sequences

Table S6: Mutation rate and 95% Confidence Intervals of phage protospacers. Mutation rates were measured using fluctuation tests (see Materials and Methods).

Name	Mutation rate	95% Confidence Interval
NC	4.9×10^{-8}	$[3.1 \times 10^{-8}, 6.7 \times 10^{-8}]$
ORF_2	1.9×10^{-7}	$[6.8 \times 10^{-8}, 3.1 \times 10^{-7}]$
ORF_5	1.1×10^{-6}	$[8.6 \times 10^{-7}, 1.3 \times 10^{-6}]$
ORF_9	1.5×10^{-7}	$[2.7 \times 10^{-8}, 2.8 \times 10^{-7}]$
ORF_17	1.6×10^{-7}	$[4.5 \times 10^{-8}, 2.8 \times 10^{-7}]$
ORF_19	1.2×10^{-6}	$[6.2 \times 10^{-7}, 1.7 \times 10^{-6}]$
ORF_20	6×10^{-7}	$[2.5 \times 10^{-7}, 9.5 \times 10^{-7}]$
ORF_21	5.7×10^{-8}	$[2.1 \times 10^{-8}, 9.2 \times 10^{-8}]$
ORF_24	4.6×10^{-8}	$[1.0 \times 10^{-8}, 8.2 \times 10^{-8}]$
ORF_27	4.3×10^{-7}	$[2.2 \times 10^{-7}, 6.5 \times 10^{-7}]$
ORF_33	4.8×10^{-8}	$[4.6 \times 10^{-9}, 9.2 \times 10^{-8}]$
ORF_37_A	7.1×10^{-7}	$[2.9 \times 10^{-7}, 1.1 \times 10^{-6}]$
ORF_37_B	5.1×10^{-7}	$[1.6 \times 10^{-7}, 8.6 \times 10^{-7}]$
ORF_38_A	1.3×10^{-7}	$[6.5 \times 10^{-8}, 1.9 \times 10^{-7}]$
ORF_38_B	2.1×10^{-7}	$[9.3 \times 10^{-8}, 1.3 \times 10^{-7}]$
ORF_38_C	9.4×10^{-9}	$[-1.2 \times 10^{-9}, 2.0 \times 10^{-8}]$
ORF_44	2.5×10^{-7}	$[5.2 \times 10^{-8}, 4.4 \times 10^{-7}]$

J. Mutation profile of escape phages

Table S7: Profile of substitutions carried by phage escape mutants. 27 substitutions are transversions and 16 are transitions.

Type of substitution	Substitution	Number of occurences
Purine Transition	A → G	6
	G → A	6
Pyrimidine Transition	C → T	1
	T → C	3
Transversion	A → C	4
	C → A	4
	A → T	7
	T → A	1
	T → G	0
	G → T	8
	G → C	1
	C → G	2

K. Escape phage relative fitness

Table S8: Relative fitness of escape phages. Deleterious mutations are highlighted in dark grey and neutral mutation in medium grey.

Phage escape mutants	Relative Fitness
2972_NC_a	0.688
2972_NC_c	-2.135
2972_NC_d	-2.072
2972_NC_e	-2.590
2972_ORF_2_a	-3.086
2972_ORF_2_b	-1.573
2972_ORF_2_c	-0.754
2972_ORF_5_a	-5.005
2972_ORF_9_a	-1.134
2972_ORF_9_b	-1.056
2972_ORF_17_a	-1.462
2972_ORF_17_b	-3.013
2972_ORF_17_d	-3.864
2972_ORF_19_a	-2.424
2972_ORF_19_b	-4.333
2972_ORF_20_b	-2.959
2972_ORF_21_a	-4.134
2972_ORF_21_c	-4.431
2972_ORF_21_d	-2.401
2972_ORF_24_c	-3.074
2972_ORF_27_a	-0.093
2972_ORF_27_d	-0.890
2972_ORF_33_a	-2.861
2972_ORF_33_b	-0.426
2972_ORF_33_c	-0.657
2972_ORF_37_A_a	-0.840
2972_ORF_37_B_a	-5.290
2972_ORF_37_B_b	0.458

Continued on next page.

Phage escape mutants	Relative Fitness
2972_ORF_37_B_c	-2.365
2972_ORF_37_B_d	-1.940
2972_ORF_38_A_a	-4.355
2972_ORF_38_A_b	-1.311
2972_ORF_38_A_e	-1.652
2972_ORF_38_B_a	0.415
2972_ORF_38_B_c	-4.282
2972_ORF_38_C_a	-3.166
2972_ORF_38_C_b	-6.212
2972_ORF_38_C_c	-2.674
2972_ORF_38_C_e	-0.215
2972_ORF_44_b	0.150

562

L. Impact of synonymous mutations on the fitness of phage escape mutants

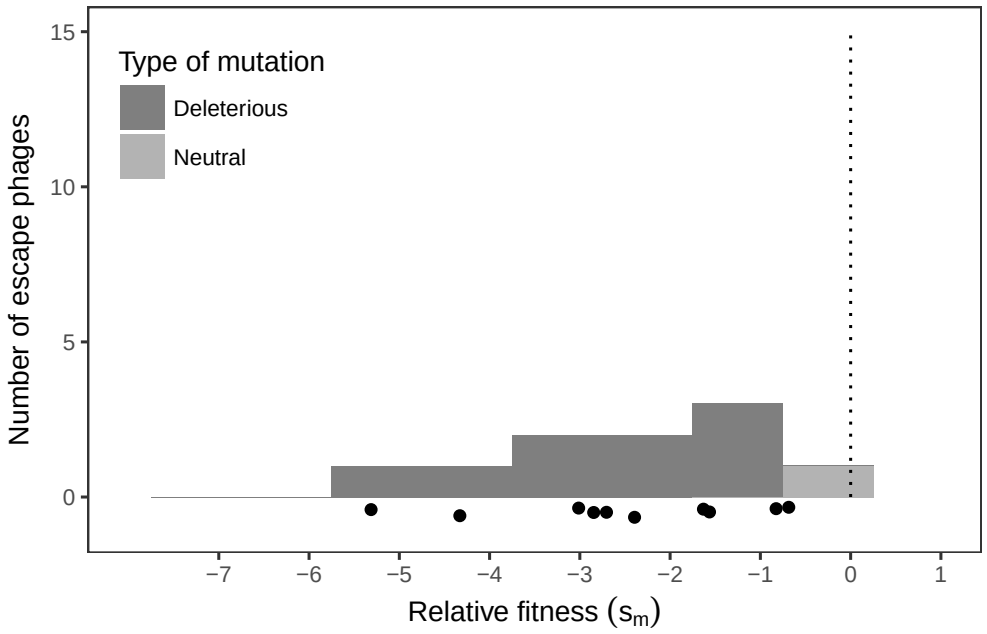

Figure S2: **Distribution of fitness effects of synonymous escape mutations in the phage.**
Relative fitness was measured through competition experiments with a collection of 10 escape phages with a synonymous mutation on their seed or PAM sequences. Phages that carry a neutral and deleterious mutations are represented in medium and dark grey respectively. Black dots show the relative fitness of each escape phage. The dotted segment represents the fitness of WT phage 2972. Fitness value of each escape phage is also provided in the supplementary informations K.